The Effect of Dark Matter During the Cosmic Dawn

M Kgoadi[1] and G Beck[1]

[1] Department of Physics, University of the Witwatersrand, Private Bag 3, WITS-2050, Johannesburg, South Africa

E-mail: kgoadimpho16@gmail.com; geoffrey.beck@wits.ac.za

Abstract. The global 21 cm signal provides rich information about the thermal and ionization history of the universe. In this work we explore how the inclusion of annihilating dark matter, specifically the Weakly Interacting Massive Particle (WIMPs) alters the global signal. To do this, we study three different WIMP masses with each having maximum allowed annihilation cross-section according to the WMAP7 observations, motivated by previous studies on this work. In our model we use updated efficiency functions as well as up-to-date temperature and ionization histories. Our model shows that DM has reduced heating effects during the cosmic dark ages and induces an absorption trough at $z \sim 25$, in distinct contrast to previous works whose results were based on earlier energy deposition efficiency models which are now believed to be substantially flawed.

1. Introduction

Dark matter (DM) forms a fundamental part of the current standard model of the Universe known as the Λ-Cold Dark Matter (ΛCDM). In this theory, about 5 % of the energy content of the Universe is made of baryonic matter, 68 % is in the form of Dark Energy and dark matter only accounts for 27 % [1]. Although the nature of DM still remains unknown, there has been numerous observations that have indirectly confirmed its existence [2, 3, 4, 5]. In this work, we focus our attention on the global 21 cm background, which is one of many ways we could constrain the nature of DM. In this scenario, DM annihilation and decay products, through the injection of high energy photons into the intergalactic medium (IGM) could heat and ionize the gas thus leaving a mark on the global signal which could be observed directly [6, 7].

In this paper we explore, in particular, the effects of WIMPs on the global 21 cm signal, with specific focus on three candidates motivated by Ref.[8]. These are 10 GeV, 200 GeV and 1 TeV WIMPs annihilating via the $b\bar{b}$ channel and have the annihilation cross-section that is compatible with the CMB observations. To get the full scope of the DM impact on the global signal, it is very important look into the details of the energy deposition from DM annihilations. Earlier studies found that a relatively small fraction of the energy deposited by DM is absorbed by the IGM and goes to ionization and heating [9]. However, recent studies have shown that DM annihilation as WIMPS can have substantial changes from the fiducial scenario with some models having twice as much heating effects as the baseline [8]. This ultimately comes down to the modelling of the energy deposition mechanisms and specifically the fraction of energy from DM that is released to or absorbed by the IGM.

We make use of a publicly available python package called Darkhistory to compute the effects of DM on the temperature and ionization history of the Universe [10]. Darkhistory allows

for fast and accurate computation of the energy deposition efficiency function $f_c(z)$ into any deposition channel c = (excitation, heating, ionization). On top of this, computing the efficiency functions with Darkhistory allows us to perform consistent calculations of the ionization and temperature histories with both exotic energy injection processes and reionization. Previous studies that have investigated the effects of DM annihilation/decay on the ionization history during the cosmic dark ages and recombination generally assumed that the injected energy from DM annihilation/decay is deposited with some redshift-independent efficiency [7, 11, 12]. It is worth noting that the calculations of these efficiency functions are very involved and we direct the readers to Refs.[10, 13, 14] for a careful and detailed analysis. To summarize, Darkhistory keeps track of the amount of the total energy from low and high energy photons and electrons deposited into the channel c. This allows the energy deposition fraction $f_c(z)$ to be calculated by normalizing the total energy deposited into the channel within a certain redshift step 1+z by the total injected energy. The annihilation byproducts will then transfer their energy into ionization and excitation of atoms, heating of the IGM and free-streaming photons to be added to the CMB continuum. The improved $f_c(z, \mathbf{x})$ functions from Darkhistory are mostly due to the fact that they are calculated with the full z and $\mathbf{x}$-dependency which was previously not done, where $\mathbf{x}$ is the ionization fractions of the relevant species in the gas denoted as $\mathbf{x} \equiv (\mathrm{x_{HII}}, \mathrm{x_{HeII}}, \mathrm{x_{HeIII}})$. This work will not indulge in the technical details and derivations of the efficiency functions but will present the equations and discuss the implications.
The structure of this paper is as follows: in section 2 we give a brief description of the 21 cm physics, in section 3 we explain in detail the DM effects on the IGM with basic equations provided. The results are provided and discussed in section 4 and we finally conclude and discuss future work in section 5.

2. 21 cm physics

The redshifted 21 cm line of hydrogen is a great probe of the epoch of reionization, this line is caused by the hyperfine transition between the singlet and triplet levels of the hydrogen ground state. The global signal is commonly described in terms of the brightness temperature and it is given by the following equation [15]

$$\delta T_b = 23\, x_{\mathrm{HI}}(z) \left(\frac{0.15}{\Omega_{\mathrm{m}}}\right)^{1/2} \left(\frac{\Omega_b h}{0.02}\right) \left(\frac{1+z}{10}\right)^{1/2} \left[1 - \frac{T_{\mathrm{R}}(z)}{T_{\mathrm{S}}(z)}\right] \mathrm{mK}, \tag{1}$$

where x_{HI} is the neutral fraction of the gas, Ω_{m} is the matter energy density and Ω_{b} is the baryon energy density. h is the hubble parameter and $T_{\mathrm{R}}(z)$ is the radiation temperature, typically assumed to be the CMB. $T_{\mathrm{S}}(z)$ is the spin temperature and is given by the ratio of the number density of hydrogen atoms in the higher energy triplet state to the lower energy singlet state which is expressed as,

$$\frac{n_1}{n_0} = \frac{g_1}{g_0} e^{-T_\star/T_{\mathrm{S}}}, \tag{2}$$

where $\mathrm{n_0}$ and $\mathrm{n_1}$ are the number densities of electrons in the singlet and triplet states respectively. The statistical weights of the energy levels are given by $g_1 = 3$ and $g_0 = 1$. $T_* = 0.0681$ K is the temperature associated with the 21 cm wavelength. In order for a signal to be detected, the spin temperature needs to deviate from the radiation background. There are three main ways that T_{S} can be determined; via the absorption or emission of 21 cm photons against the CMB, through resonant scattering of Lyman-α photons which cause downward transitions from the triplet state to the singlet state via the Wouthuysen-Field effect and lastly, through the collisions with electrons and other hydrogen atoms (See [16] for an extensive overview). The spin temperature at these limits can be written as [17]

$$T_S^{-1} = \frac{T_{\rm CMB}^{-1} + x_\alpha T_\alpha^{-1} + x_c T_K^{-1}}{1 + x_\alpha + x_c}, \tag{3}$$

where $T_{\rm CMB}$ is the background temperature, $\rm T_\alpha$ is the color temperature associated with the Lyman-α radiation field and is closely coupled to the kinetic temperature $\rm T_K$ [18]. The coupling coefficients for collisions and scattering of Lyman-α photons are given by $\rm x_c$ and $\rm x_\alpha$ respectively and are given by the following expressions:

$$x_\alpha = \frac{16\pi\sigma_\alpha T_* J_\alpha}{27 A_{10} T_k E_\alpha}, \tag{4}$$

$$x_c = \frac{(k_{10} n_{\rm HI} + n_{\rm e}\gamma_{\rm e}) T_*}{A_{10} T_k}, \tag{5}$$

where $A_{10} = 2.85 \times 10^{-15}$ $\rm s^{-1}$ is the coefficient for spontaneous emission of the 21 cm line, J_α is the Lyman-α emissivity, k_{10} is the tabulated temperature data from [19]. The coupling coefficients determine whether collisions or Lyman-α photons affect the signal and provides information about how strongly coupled is the spin temperature to the gas temperature. This means that the signal will appear as absorption or emission if either the collisions or the Lyman-α radiation couples the spin temperature to the kinetic temperature. The equation that has a contribution from DM annihilation is given by,

$$J_{\alpha,\rm DM} = \frac{hcn_{\rm H}^2(z)}{4\pi H(z)} f_{c,\alpha} \frac{E_{\rm DM}}{\rm n_H E_\alpha}, \tag{6}$$

where $f_{c,\alpha}$ is the fraction of annihilation energy that goes into Lyman-α excitation, n_H represents the hydrogen atom number density, E_α is the Lyman-α excitation energy and E_{DM} is the energy rate from DM annihilation. The next section will address the significance of the efficiency fractions in the context of energy deposition by DM into the IGM.

3. Exotic energy injection on the IGM

Next, we shift our focus on the implications of DM annihilations on the thermal and ionization evolution of the IGM, which directly determines the changes of the global 21 cm signal. It is thought that DM annihilation in the early Universe can act as a source of X-rays which lead to ionization, heating and other processes [20]. DM annihilation rate scales as the square of the density, n_{DM}^2 , this indicates that it rises with the onset of structure formation and that the collapse of DM into halos can have a significant energy injection in the process of reionization. The rate of energy injection from DM annihilation or decay is given by [10]

$$\left(\frac{dE}{dV dt}\right)^{\rm inj} = \begin{cases} \rho_{\chi,0}^2 (1+z)^6 \langle\sigma v\rangle / m_\chi, & \text{annihilation,} \\ \rho_{\chi,0}(1+z)^3/\tau, & \text{decay,} \end{cases} \tag{7}$$

where m_χ is the mass of DM, $\langle\sigma v\rangle$ is the velocity averaged cross-section, τ is the decay lifetime and $\rho_{\chi,0}$ is the mass density of DM today. Annihilation and decay products have the potential to alter the levels of ionization, can heat up neutral gas and increase the production of Lyman-α photons. The evolution of the free electron fraction and the matter temperature is given by [11]

$$-\frac{dx_e}{dz} = \frac{1}{H(z)(1+z)}[R_s(z) - I_s(z) - I_x(z)], \tag{8}$$

and

$$(1+z)\frac{dT_k}{d_z} = 2T_k - \kappa_s(z) - \kappa_x(z), \tag{9}$$

where R_s, I_s are the standard recombination and ionization rates. The standard heating is given by κ_s. I_x and κ_x are the dark matter contributions to the ionization and heating. The ionization rate I_x and heating κ_x from DM are given by

$$I_x(z) = f_{c,\mathrm{ion}}(z)\,\frac{m_{\mathrm{DM}}}{E_0}\,n_{\mathrm{DM}}^2\,\langle\sigma V\rangle\,, \tag{10}$$

and

$$\kappa_x(z) = \frac{f_{c,\mathrm{heat}}(z)\,m_{\mathrm{DM}}\,n_{\mathrm{DM}}^2\,\langle\sigma V\rangle}{3\,k_B\,H(z)\,(1+f_{\mathrm{He}}+x_e(z))}, \tag{11}$$

where m_{DM} is the mass of the DM particle, $E_0 = 13.6$ eV is the threshold ionization of hydrogen, k_B is the Boltzmann factor, $\langle\sigma V\rangle$ is the annihilation cross-section, $H(z)$ is the Hubble parameter and f_{He} is the helium fraction. The functions $f_{\mathrm{c,ion}}(z)$ and $f_{\mathrm{c,heat}}(z)$ are the fractions of annihilation energy that go into ionization and heating respectively. The energy deposited into any channel c can be parametrized as [10]

$$\left(\frac{dE}{dVdt}\right)_c^{\mathrm{dep}} = f_c(z,x)\left(\frac{dE}{dVdt}\right)^{\mathrm{inj}}, \tag{12}$$

with all the complicated physics condensed into a factor that depends on redshift and the ionization fraction of all the relevant species in the gas. Darkhistory goes into all the details needed to calculate the efficiency function $f_c(z,x)$ but provides the resulting modifications to T_k and x_e with DM energy injection as

$$T_k = \frac{2f_{\mathrm{heat}}(z,x)}{3(1+F_{\mathrm{He}}+x_e)n_{\mathrm{H}}}\left(\frac{dE}{dVdt}\right)^{\mathrm{inj}}, \tag{13}$$

$$x_e = \left[\frac{f_{\mathrm{H_{ion}}}(z,x)}{R_{\mathrm{n_H}}} + \frac{(1-C)f_{\mathrm{exc}}(z,x)}{0.75R_{\mathrm{n_H}}}\right]\left(\frac{dE}{dVdt}\right)^{\mathrm{inj}}, \tag{14}$$

where $R_{\mathrm{n_H}}$ is the hydrogen ionization potential, $F_{He} = n_{He}/n_H$ is the helium abundance, n_H is the number density of hydrogen, $f_{\mathrm{exc}}(z,x)$ is the fractions of annihilation energy that go into excitation and C is the Peebles-C factor which is the probability of HI in the n = 2 state decaying to the ground state. The results of Darkhistory are then used to compute the global 21 cm signal following equations Equation 1 - Equation 6.

4. Results

We present the results obtained for the three DM models in section 1. The associated masses have the maximum allowed values according to the CMB observations; for 200 GeV the annihilation cross-section is $\langle\sigma v\rangle_{\mathrm{max}} = 1.2 \times 10^{-24}$ cm^{3}s^{-1}, for 10 GeV the annihilation cross-section is $\langle\sigma v\rangle_{\mathrm{max}} = 1 \times 10^{-25}$ cm^{3}s^{-1} and for 1 TeV the annihilation cross-section is $\langle\sigma v\rangle_{\mathrm{max}} = 1.4 \times 10^{-23}$ cm^{3}s^{-1}. These were chosen to see how the DM predictions change with the efficiency functions from Darkhistory, the models were kept the same as [8] for the purpose of comparison. We compare our results to the baseline, which is the default signal without DM. It is worth pointing out that our analysis does not include the astrophysical sources below z $\sim$ 30, this follows the analysis of Ref.[6]. This is done so that we can easily study the DM effects on the global signal. The baseline model uses reionization models from [21] and is consistent with rapid reionization. This model provides photoheating and photoionization rates as functions of redshift.

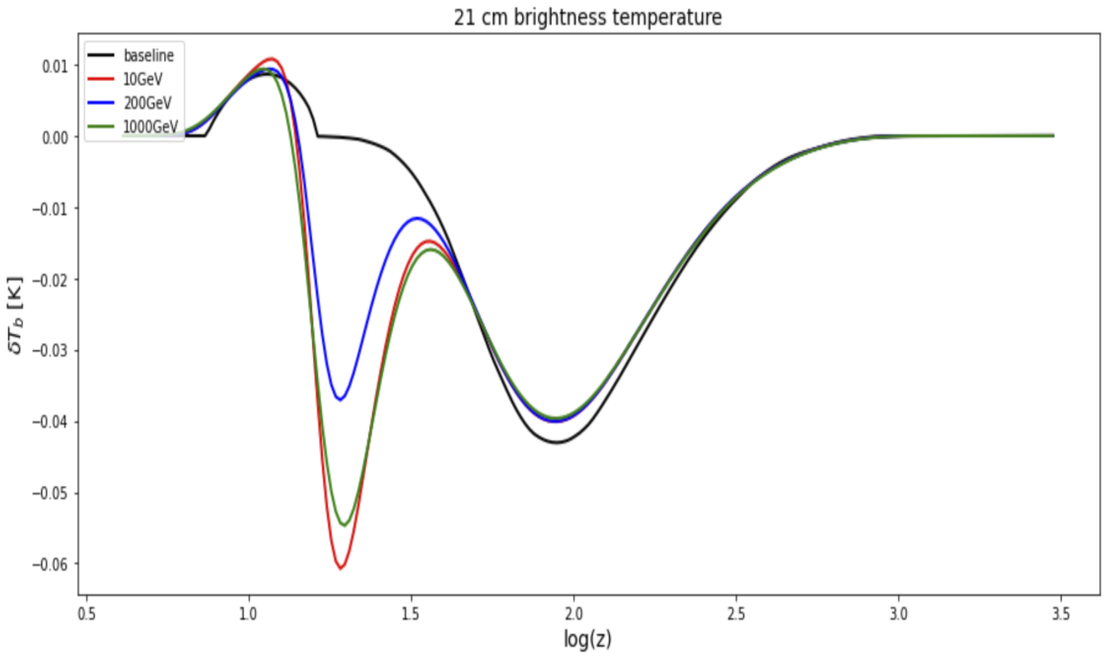

Figure 1. The brightness temperature as a function of redshift in a $\log_{10}$ scale, for all the considered DM models. The baseline case without any injected energy from DM annihilation is depicted in the black line. The red line is for a 10 GeV DM mode with a $b\bar{b}$ channel, the blue line depicts the 200 GeV DM with W^+W^- channel and finally the green line is the 1000 GeV DM with $\mu^+\mu^-$ annihilation channel.

Before we dive into the analysis, we note that in Figure 1, the smoothing of the plots is not a DM related effect. We also notice that the results do not scale up with mass. Another important factor is that the models chosen are have different annihilation channels which suggests that there is more at play than just $\langle\sigma v\rangle$ and m_χ. The efficiency functions vary depending on the nature of the annihilation products. Varying the mass will change the composition of the products and complicate naive expectations. Now looking at $z \sim 100$, during the Cosmic Dark Ages, we see that there is a reduction in the absorption trough for the DM case compared to the baseline because DM is heating the neutral hydrogen at this period and this causes emission, albeit very small. This is because the kinetic temperature at these redshifts is increasing since there is a high density of DM and therefore higher chance of annihilations. It is worth noting that in [8], the various DM models they use reduce this trough quite substantially compared to ours. Looking at one example; 10 GeV WIMP, we see that the difference of our model compared to the baseline is about 5 mK whereas in [8], they produce a difference of about 10 mK, this is twice as much as what we produce for the same mass. This is due to the updated efficiency function f_c that is provided by Darkhistory. When we look to $z \sim 30$, we notice that instead of heating and reducing the absorption trough as seen in [8], we are inducing an absorption feature in the case of DM. The 10 GeV model produces lower energy products, compounded by the smaller cross-section, this reduces heating efficiency. The 1 TeV model experiences a far larger cross-section but is suppressed by reduced number density. The 200 GeV case benefits from a larger cross-section than 10 GeV and doesn't carry as large a number density suppression as 1 TeV. Now moving to the onset of reionization, we see that our model, especially 10 GeV increases the emission very slightly at z $\sim$ 10. This means that the efficiency functions we used produces opposite effects to previous studies in this topic, as can be seen with the surprisingly

strong absorption features.

5. Conclusion and future work

In this work we presented an argument for the use of a comprehensive approach of investigating the effect of dark matter in the early universe using the redshifted 21 cm hydrogen line. It is important to note that the work done here has limitations in a sense that there were no astrophysical sources included at $z \leq 30$, meaning that the results obtained are for optimistic cases. We have seen that studying the early universe with particular focus on the global 21 cm signal is a great probe of exotic energy injection. However, this requires precise modelling of the energy deposition especially the efficiency functions and the physics within them. Our results have shown that previous assumptions of f_c were highly over-estimated and Darkhistory lets us correct this.

The early results are promising but more work still needs to be done. Firstly, we need to add the astrophysical sources of Lyman-α and X-rays at the on-set of the Cosmic Dawn. This will allow us to have a full picture of the global 21 cm signal. Further work will investigate the potential for detecting or constraining DM annihilation effects using single-dish experiments and potentially interferometers.

Acknowledgments

M.K acknowledges support from a National Research Foundation of South Africa Thuthuka grant no. 117969.

References

[1] Aghanim N, Akrami Y, Ashdown M, Aumont J, Baccigalupi C, Ballardini M, Banday A, Barreiro R, Bartolo N, Basak S *et al.* 2020 *Astronomy & Astrophysics* **641** A6
[2] Ade P A, Aghanim N, Arnaud M, Ashdown M, Aumont J, Baccigalupi C, Banday A, Barreiro R, Bartlett J, Bartolo N *et al.* 2016 *Astronomy & Astrophysics* **594** A13
[3] Blumenthal G, Faber S, Primack J and Rees M 1985 *Nature* **313** 72
[4] Clowe D, Gonzalez A and Markevitch M 2004 *The Astrophysical Journal* **604** 596
[5] Schramm D N and Turner M S 1998 *Reviews of Modern Physics* **70** 303
[6] Valdes M, Ferrara A, Mapelli M and Ripamonti E 2007 *Monthly Notices of the Royal Astronomical Society* **377** 245–52
[7] Furlanetto S R, Oh S P and Pierpaoli E 2006 *Physical Review D* **74** 103502
[8] Valdés M, Evoli C, Mesinger A, Ferrara A and Yoshida N 2013 *Monthly Notices of the Royal Astronomical Society* **429** 1705–16
[9] Ripamonti E, Mapelli M and Ferrara A 2007 *Monthly Notices of the Royal Astronomical Society* **374** 1067–77
[10] Liu H, Ridgway G W and Slatyer T R 2020 *Physical Review* D **101** 023530
[11] Chen X and Kamionkowski M 2004 *Physical Review* D **70** 043502
[12] Mapelli M, Ferrara A and Pierpaoli E 2006 *Monthly Notices of the Royal Astronomical Society* **369** 1719–24 ISSN 1365-2966 URL `http://dx.doi.org/10.1111/j.1365-2966.2006.10408.x`
[13] Slatyer T R, Padmanabhan N and Finkbeiner D P 2009 *Physical Review* D **80** 043526
[14] Slatyer T R 2013 *Physical Review* D **87** 123513
[15] Zaldarriaga M, Furlanetto S R and Hernquist L 2004 *The Astrophysical Journal* **608** 622
[16] Pritchard J R and Loeb A 2012 *Reports on Progress in Physics* **75** 086901
[17] Furlanetto S R, Oh S P and Briggs F H 2006 *Physics reports* **433** 181–301
[18] Field G B 1959 *The Astrophysical Journal* **129** 536
[19] Allison A and Dalgarno A 1969 *The Astrophysical Journal* **158** 423
[20] Liu H, Slatyer T R and Zavala J 2016 *Physical Review D* **94** 063507
[21] Puchwein E, Haardt F, Haehnelt M G and Madau P 2019 *Monthly Notices of the Royal Astronomical Society* **485** 47–68 ISSN 1365-2966 URL `http://dx.doi.org/10.1093/mnras/stz222`